JBC Papers in Press. Published on September 30, 2009 as Manuscript M109.059022
The latest version is at http://www.jbc.org/cgi/doi/10.1074/jbc.M109.059022

# MUTATIONS IN ARABIDOPSIS FATTY ACID AMIDE HYDROLASE REVEAL THAT CATALYTIC ACTIVITY INFLUENCES GROWTH BUT NOT SENSITIVITY TO ABSCISIC ACID OR PATHOGENS*

**Sang-Chul Kim[1], Li Kang[2], Satish Nagaraj[2], Elison B. Blancaflor[1,2], Kirankumar S. Mysore[2,a], and Kent D. Chapman[1,a]**

[1]Center for Plant Lipid Research, Department of Biological Sciences, University of North Texas, Denton, TX 76203 USA
[2]Plant Biology Division, Samuel Roberts Noble Foundation, Ardmore, OK 73402 USA

Running head: AtFAAH functions independent of catalytic activity

[a]Joint correspondence: Kent D. Chapman, Ph.D., University of North Texas 1155 Union Circle, #305220 Denton, TX 76203-5017. Tel: 940-565-2969; Fax: 940-369-8656; E-mail: chapman@unt.edu; Kirankumar S. Mysore, Ph.D., Samuel Roberts Noble Foundation, 2510 Sam Noble Pky., Ardmore, OK 73401. Tel: 580-224-6740; E-mail: ksmysore@noble.org

Downloaded from www.jbc.org by guest, on July 11, 2010

## ABSTRACT

**Fatty acid amide hydrolase (FAAH) terminates the endocannabinoid signaling pathway that regulates numerous neurobehavioral processes in animals by hydrolyzing *N*-acylethanolamines (NAEs). Recently, an Arabidopsis FAAH homologue (AtFAAH) was identified, and several studies, especially those using *AtFAAH*- overexpressing and knockout lines, have suggested an *in vivo* role for FAAH in the catabolism of NAEs in plants. We previously reported that the overexpression of AtFAAH in Arabidopsis resulted in accelerated seedling growth, and in seedlings that were insensitive to exogenous NAEs but hypersensitive to abscisic acid (ABA) and hypersusceptible to nonhost pathogens. Here we show that while the enhanced growth and NAE tolerance of the AtFAAH-overexpressing seedlings depend on the catalytic activity of AtFAAH, hypersensitivity to ABA and hypersusceptibility to nonhost pathogens are independent of its enzymatic activity. Five amino acids known to be critical for rat FAAH activity are also conserved in AtFAAH (K205, S281, S282, S305, and R307). Site-directed mutation of each of these conserved residues in AtFAAH abolished its hydrolytic activity when expressed in *E. coli*, supporting a common catalytic mechanism in animal and plant FAAH enzymes. Overexpression of these inactive AtFAAH mutants in Arabidopsis showed no growth enhancement and no NAE tolerance, but still rendered the seedlings hypersensitive to ABA and hypersusceptible to nonhost pathogens to a degree similar to the overexpression of the native AtFAAH. Taken together, our findings suggest that the AtFAAH influences plant growth and interacts with ABA signaling and plant defense through distinctly different mechanisms.**

## INTRODUCTION

Fatty acid amide hydrolase (FAAH) catalyzes the hydrolysis of acylethanolamides, such as *N*-acylethanolamines (NAEs) (1-4), as well as fatty acid primary amides (5-7). FAAH is known to terminate the "endocannabinoid" signaling pathway that regulates a variety of neurobehavioral processes in animals (reviewed in (8-10)). This membrane-bound protein is a member of an enzyme superfamily termed the "amidase signature" (AS) family (11-12). Members of the AS family (more than 80 amidases) are characterized by a highly conserved region that consists of ~130 amino acids rich in serine, glycine and alanine residues (11-16). The x-ray crystal structure of rat FAAH revealed that the core catalytic machinery of FAAH, in contrast to the Ser-His-Asp triad typical of most serine hydrolases, consists of a novel Ser-Ser-Lys



Copyright 2009 by The American Society for Biochemistry and Molecular Biology, Inc.

catalytic triad (12,17-19). FAAH (-/-) knockout mice had higher endogenous levels of NAEs compared to wild-type mice, and exhibited a variety of physiological and behavioral abnormalities in response to endocannabinoids, such as hypomotility, analgesia, catalepsy, and hypothermia (20-23). These observations suggested that FAAH was a key enzyme involved in the catabolism of NAEs *in vivo* and was responsible for termination of the endocannabinoid signaling.

In plants, FAAH homologues were identified and characterized recently at the biochemical level (24-25), but much remains to be learned regarding the precise cellular function and physiological significance of this enzyme in plants. An NAE hydrolase activity was first detected *in vitro* in homogenates of tobacco cells (26), and was demonstrated both *in vivo* and *in vitro* in imbibed cotton seeds through radiolabeling approaches (27). An Arabidopsis FAAH homologue (*AtFAAH*; locus At5g64440) was identified that encodes a protein of 607 amino acids with 37 % identity to rat FAAH within the AS domain (24). Catalytic residues (Lys205, Ser281 and Ser305) were absolutely conserved and a single transmembrane domain, like rat FAAH, was predicted to be present near N-terminus of the protein (24). Recombinant protein, expressed in *E. coli*, was indeed active in hydrolyzing a variety of naturally occurring fatty acid amides (24). Functional FAAH homologues have been identified and characterized in diverse plant species (25). Homology modeling of the AS region of the plant FAAH revealed a highly conserved active site organization with the catalytic triad positioned in the substrate-binding site (25).

Several lines of evidence, especially those using *AtFAAH*- overexpressing and T-DNA insertion mutant plants, clearly support a role for FAAH *in vivo* in the catabolism of NAEs in plants. Exogenous NAE at low micromolar concentrations exhibited a dose-dependent reduction of Arabidopsis seedling growth (28), suggesting that hydrolysis of endogenous NAEs by AtFAAH might be important for normal development. Indeed, AtFAAH overexpressors displayed enhanced seedling growth and increased cell/organ size (29). Seeds of AtFAAH overexpressors had lower endogenous NAE content, and their seedling growth was less sensitive to exogenous NAE, whereas *AtFAAH* knockout seeds had elevated levels of endogenous NAEs in desiccated seeds, and their seedlings were hypersensitive to exogenous NAE (29). These results suggested that FAAH is a modulator of endogenous NAE levels in plants and that NAE turnover by the action of FAAH likely participates in the regulation of plant growth.

Recently, AtFAAH overexpressors have exhibited several additional intriguing phenotypes. Overexpression of AtFAAH resulted in seedlings that were hypersensitive to the growth inhibitory effects of a plant hormone abscisic acid (ABA) (30). AtFAAH overexpressors were also found to be hypersusceptible to several bacterial pathogens and nonhost pathogens compared with wild-type plants, and this was attributed, in part to alterations in phytohormone accumulation and signaling (31). Interestingly, however, these phenotypic effects did not seem to be directly attributed to NAE turnover by AtFAAH. Even though AtFAAH overexpressors were compromised in innate immunity compared to wild-type plants, their NAE content and compositions in mature leaves were similar to those of wild-type plants (31). Likewise, application of ABA on AtFAAH overexpressors resulted in a marked reduction in growth despite little difference in NAE content or composition between ABA-treated and untreated seedlings (30).

Because FAAH is able to hydrolyze other types of lipid substrates *in vitro* (like monoacylglycerols (32-34) and fatty acid primary amides (5-7,34)), it is possible that AtFAAH-mediated hydrolysis of other endogenous substrates, yet to be identified, may explain this enzyme's impact on interaction with plant defense and ABA signaling, separate from its role in NAE catabolism. Here we test this possibility by ectopic overexpression of catalytically inactive, site-directed mutant forms of AtFAAH in Arabidopsis and examining the resulting effects on growth, ABA sensitivity and innate immunity. As expected, overexpression of the AtFAAH variants without catalytic activities led to no growth enhancement and no NAE tolerance. Interestingly the transgenic AtFAAH variant lines remained hypersensitive to ABA and hypersusceptible to nonhost pathogens despite lack of enzymatic activity. Consequently, our findings suggest that AtFAAH possesses at

Downloaded from www.jbc.org by guest, on July 11, 2010

least two co-existing activities. It influences plant growth through its amidase activity toward NAEs, while interacting with plant defense and ABA signaling through other, unknown mechanisms independent of its catalytic activity.

## EXPERIMENTAL PROCEDURES

*Chemicals and reagents*- [1-$^{14}$C]Lauric acid was purchased from Amersham Biosciences (Alameda, CA). [1-$^{14}$C]Palmitic acid and [1-$^{14}$C]linoleic acid were from DuPont NEN (Boston, MA). Dimethylsulfoxide (DMSO), isopropyl β-D-1-thiogalactopyranoside (IPTG), ethanolamine, *cis*-9-octadecenamide, and abscisic acid (ABA) were from Sigma-Aldrich (St. Louis, MO). Silica gel G (60 Å)-coated glass plates (10×20 cm or 20×20 cm, 0.25 mm thickness) were from Whatman (Clifton, NJ). *n*-Dodecyl β-D-maltoside (DDM) was from Calbiochem (La Jolla, CA). All organic solvents (isopropanol, chloroform, hexane, ethylacetate, and methanol) were from Fisher Scientific (Fair Lawn, NJ). PVDF membrane (0.2 μm) and goat anti-mouse (or anti-rabbit) IgG conjugated to horseradish peroxidase were from Bio-Rad (Hercules, CA). Anti-c-Myc monoclonal antibody was from Abgent (San Diego, CA). Anti-AtFAAH polyclonal antibody was generated in Biosynthesis (Lewisville, TX). *N*-lauroyl ethanolamide, *N*-palmitoyl ethanolamide, *N*-linoleoyl ethanolamide, and *sn*-2-arachidonoyl glycerol were from Cayman Chemical (Ann Arbor, MI).

*Plant materials and growth measurements*- *AtFAAH* T-DNA insertional mutant (SALK_095108) was originally obtained from the Arabidopsis Biological Resource Stock Center (Ohio State University, Columbus, OH) and was characterized previously (29). Transgenic Arabidopsis lines overexpressing native AtFAAH proteins under the control of the cauliflower mosaic virus (CaMV) 35S promoter were previously described (29). Plants were screened for zygosity using REDExtract-N-Amp Plant PCR kit (Sigma-Aldrich, St. Louis, MO). Plants were propagated in soil for seed production. For growth assay, seeds were first surface-sterilized with 95 % ethanol, 30 % bleach containing 0.1 % Tween-20 and deionized water, and stratified for 3 days at 4 °C in the dark. Seeds were grown for 10 days in nutrient media (0.5x Murashige and Skoog salts containing 1 % sucrose) in a controlled environment room with a 16-h-light/8-h-dark cycle at 20 °C. For detailed growth measurements, seedlings grown on agar plates were tilted at ~60° angle to facilitate reproducible measurements of root elongation. Cotyledon area and primary root length were measured from captured images of the seedlings. For fresh weight measurements, seedlings were grown in liquid media with shaking at 75 rpm, harvested by filtration, dried, and quantified in terms of seedling mass (mg) normalized to mass of seeds sown (mg). ABA or NAE, both dissolved in dimethylsulfoxide (DMSO), were added to the appropriate final concentrations, and untreated controls contained equivalent amount of DMSO alone (always less than 0.05 % by volume). Concentrations of exogenous ABA were calculated based on the active *cis*-isomer. For pathogen assays, the plants were grown in short day conditions (10-h-light/14-h-dark cycle), with day temperature of 21 °C and night temperature of 19 °C at a relative humidity of 70 %.

*Site-directed mutagenesis of AtFAAH*- The original construct pCAMBIA1390-*AtFAAH* used to generate overexpressor lines (29) was used as template in reactions of site-directed mutagenesis by using QuikChange® II XL site-directed mutagenesis kit according to the manufacturer's recommendations (Stratagene, La Jolla, CA). In short, 50 ng of the template DNA was used in PCR reactions with primers containing nucleotide corresponding to amino acid change. The PCR program includes the following steps: 95 °C for 1 min, (95 °C for 50 sec, 60 °C for 50 sec, 68 °C for 12 min) repeat 17 more cycles, and 68 °C for 7 min. The reaction mix was digested with DpnI at 37 °C for 2 hours to remove parent plasmids. Then the DNA was precipitated and used to transform XL10-Gold competent cells. Mutations were confirmed by sequencing. The constructs were transformed into *Agrobacterium* strain GV3101 and used to transform Arabidopsis wild-type (Col-0) and *AtFAAH* knockout plants by floral-dipping (35). Transgenic plants resistant to hygromycin (15 mg/L) were selected from MS medium. Putative transgenic plants were further confirmed with sequencing and RT-PCR with construct specific primers.

*Recombinant protein expression and purification*- For proteins expressed in *E. coli*,

Downloaded from www.jbc.org by guest, on July 11, 2010

*AtFAAH* cDNAs with the site-directed mutations were PCR-amplified, agarose gel-purified, cloned into pTrcHis2 vector (Invitrogen, Carlsbad, CA), and transformed into *E. coli* TOP10 cells. Selected transformants were grown in LB medium at 37 ºC with shaking at 250 rpm to an $OD_{600}$ of 0.6, and incubated with 1 mM IPTG for 4 h. Recombinant proteins expressed in frame with 6X His tag were nickel-nitrilotriacetic acid (Ni-NTA) affinity-purified using QIAexpress protein purification kit (Qiagen, Valencia, CA) according to manufacturer's instructions. Eluted proteins were concentrated, and imidazole was removed with 50 mM Tris-HCl (pH8.0), 100 mM NaCl, and 0.2 mM dodecylmaltoside (DDM) by filtration-centrifugation using Centricon YM-30 (Millipore, Bedford, MA). Protein concentrations were determined by Bradford assay using BSA as a standard. For proteins expressed in Arabidopsis, seedlings grown in liquid media were flash frozen and powdered in liquid nitrogen using a mortar and pestle, and suspended in homogenization buffer (100 mM potassium phosphate, pH7.2, 400 mM sucrose, 10 mM KCl, 1 mM EDTA, 1 mM EGTA, 5 mM $MgCl_2$). After incubation on ice for 30 min, homogenates were centrifuged at 12,000 xg for 15 min, and resulting supernatants were used for further experiments.

*FAAH enzyme activity assays*- $^{14}C$-radiolabeled NAEs were synthesized from corresponding free fatty acids and ethanolamine (27), and combined with non-radiolabeled NAEs to achieve desired final concentration. Enzyme activity was determined based on radiospecific activity. Protein samples were incubated with 100 μM (~12,000 cpm) NAEs (12:0, 16:0, or 18:2) or 100 μM 2-arachidonoyl glycerol in 50 mM Bis-Tris buffer (pH9.0) in a final volume of 0.4 mL at 30 °C for 30 min with shaking at 120 rpm. Reactions were terminated by the addition of boiling isopropyl alcohol (70 °C) for 30 min. Total lipids were extracted into chloroform, washed twice with 1M KCl and once with water, and separated by Silica gel-thin layer chromatography (TLC) using an organic solvent mixture of hexane, ethyl acetate and methanol (60:40:5 v/v/v). Distribution of unreacted substrates and products formed was evaluated either by radiometric scanning (AR-2000 Imaging Scanner, Bioscan, NW Washington, DC) of the TLC plate for amidase activity assays or by exposure of the plate to iodine vapors for monoacyl esterase activity assays.

*Western blot analysis*- Protein samples were separated on 10 % polyacrylamide/SDS gels and electrophoretically transferred onto polyvinylidene fluoride (PVDF) membranes in a Semidry-Trans-Blot apparatus (Bio-Rad, Hercules, CA) for 30 min at constant 14 V. The membranes were blocked in 5 % nonfat milk in Tris-buffered saline (20 mM Tris-HCl, pH7.5 and 500 mM NaCl) containing 0.1 % Tween-20. Affinity-purified proteins expressed in *E. coli* as in-frame c-Myc-epitope fusions and proteins expressed in Arabidopsis were localized by overnight incubation at room temperature with mouse monoclonal anti-c-Myc antibodies (Abgent, San Diego, CA) or rabbit polyclonal anti-AtFAAH antibodies, respectively. Immunolocalized proteins were detected by chemiluminescence following incubation for 1 h at room temperature with either goat anti-mouse IgG or goat anti-rabbit IgG (Bio-Rad, Hercules, CA), both conjugated to horseradish peroxidase, according to manufacturer's instructions.

*Pathogen assay*- The pathogen growth assay was performed as previously described (31) whereby, *Pseudomonas syringae* pv. *tabaci* was grown in Kings B agar (KB) medium with appropriate antibiotics for 16 h at 30 °C. The cells were pelleted by centrifugation at 3000 xg, washed three times and resuspended in sterile water for inoculation. Bacterial suspension was syringe-infiltrated into leaves at a concentration of $5 \times 10^7$ cfu/mL for symptom development, and was vacuum-infiltrated with a concentration of $10^7$ cfu/mL for growth assays. Leaf disks of approximately 1 $cm^2$ were taken from inoculated leaves, homogenized in sterile water and the serial dilutions of the samples were plated onto KB agar plates.

## RESULTS

*Site-directed mutagenesis of AtFAAH.* Site-directed mutagenesis studies of rat FAAH identified five amino acids (Lys142, Ser217, Ser218, Ser241, and Arg243), including and nearby the catalytic triad, where substitution to alanine significantly decreased catalytic activity of the protein (19). Amino acid sequence alignment between rat and Arabidopsis FAAH proteins over

Downloaded from www.jbc.org by guest, on July 11, 2010

the entire AS domain showed that the residues critical for the rat FAAH activity were absolutely conserved in AtFAAH sequence (Lys205, Ser281, Ser282, Ser305, and Arg307; Fig. 1). Therefore, the corresponding residues in AtFAAH could also be critical for its amidase activity.

We performed a systematic mutational analysis for each of the five conserved residues of AtFAAH by converting them to alanine to evaluate their importance for catalytic activity and biological functions in development and stress responses. Since Ser281 and Ser282 are located adjacent to each other on the protein molecule, a S281/282A double mutant was generated to rule out the possibility that mutation of one of the two serine residues might compromise catalytic activity by structurally impacting the other residue. As a control, a S360A mutation was also generated since it is outside the amidase signature sequence and should have no impact on catalysis. Thus, the following mutants were generated for this study and expressed as recombinant proteins for functional analysis in *E. coli*: K205A, S281/282A, S305A, R307A, and S360A. Western blot analysis using affinity-purified proteins with the mutations showed that the proteins are normally expressed in *E. coli* in roughly similar levels (Fig. 1B).

*Mutations in the amidase domain of AtFAAH abolished enzyme activity.* When NAE hydrolase assays were performed with equal amounts of affinity-purified, mutated proteins using NAE16:0 as a substrate, no detectable amount of the product (free fatty acid 16:0) was found in K205A, S281/282A, S305A, and R307A mutants, whereas S360A mutant exhibited fairly similar level of product formation to wild-type (native) protein (Fig. 1C), providing a negative control for comparison. Based on the assay results, specific activities for the mutants and their relative activities to wild-type protein were calculated and summarized in table 1. Kinetic comparisons between wild-type AtFAAH and S360A mutant showed that the mutation outside the FAAH active site had similar kinetic properties and catalytic efficiencies ($K_{cat}/K_m$) toward NAE substrates as the native FAAH (Fig. 1D and Table 2).

Enzyme activity assays were also conducted with NAE12:0, NAE18:2, a fatty acid primary amide, 9-octadecenamide (oleamide), and a monoacylglycerol, 2-arachidonylglycerol (2-AG), to test the mutant enzymes against a broad range of substrate types including long and short-chain acylamides, long chain polyunsaturated acylamides, primary amides, and monoacylesters (Fig. 1). These substrates were all hydrolyzed well by wild-type AtFAAH, but were hydrolyzed to barely detectable degree by the site-directed mutants, except for S360A mutant that exhibited similar activity to wild-type protein for all the substrates tested (Fig. 1E and Table 1). Overall, all AtFAAH mutants displayed slightly better activities toward long chain polyunsaturated NAEs, and R307A mutant hydrolyzed all the NAE substrates better than the other mutants did (Table 1). These results suggest that the five residues reported to be important for activity of rat FAAH (19), are also essential for the hydrolase activity of AtFAAH, and support a common catalytic mechanism of animal and plant FAAH enzymes.

*Overexpression of the site-directed mutant AtFAAH proteins in Arabidopsis.* To test the impact of NAE turnover, or of hydrolysis of unknown lipid substrates by AtFAAH overexpressors, catalytically "dead" enzymes were overexpressed in wild-type and *AtFAAH* knockout backgrounds. *AtFAAH* cDNAs with K205A, S281/282A, S305A, and R307A cloned in pCAMBIA-1390 vector were used to transform Arabidopsis wild-type (Col-0) and the *AtFAAH* knockout mutant using floral dip transformation (35). Transgenic plants were successfully obtained for S281/282A and R307A mutants. Western blot analysis using homogenates of 10-day old seedlings showed that S281/282A and R307A mutant lines overexpressed their respective mutated proteins (Fig. 2A). The two backgrounds for transformation allowed for the endogenous AtFAAH to be accounted for. AtFAAH protein was essentially undetectable in homogenates of wild-type and *AtFAAH* knockout plants; the protein exists in very low abundance in wild-type, and it was barely detected in immunoblots of isolated microsomes prepared from homogenates of wild-type plants (not shown).

When NAE hydrolase assays were performed with equal amounts of total proteins extracted from 10-day old seedlings using NAE16:0 as a substrate, both S281/282A and R307A mutants transformed into the wild-type background exhibited slightly reduced activities compared to wild-type plants alone, presumably

Downloaded from www.jbc.org by guest, on July 11, 2010

due to the competition for substrate binding between the active and inactive enzymes (Fig. 2B; (25)). However, both of these two site-directed mutants exhibited significantly lower enzyme activity than overexpression of the native AtFAAH, clearly distinguishing the expression of site-directed mutant forms from overexpression of authentic AtFAAH. As expected, no measurable activity was found when either of the mutant forms were transformed into the *AtFAAH* knockout plants (Fig. 2B), despite protein accumulation detected on western blots (Fig. 2A).

*AtFAAH enzyme activity is required for enhanced seedling growth observed in AtFAAH overexpressing plants.* To ask whether NAE hydrolase activity of AtFAAH was required for enhanced seedling growth (29-30), growth phenotypes of 10-day old seedlings of the site-directed mutant lines in response to NAE12:0 were determined by measuring their seedling fresh weights, primary root lengths, and cotyledon areas. Generally, both S281/282A and R307A mutants exhibited growth phenotypes essentially identical to those of their background lines (Col-0 and *AtFAAH* knockout) when treated with either solvent (DMSO) only or NAE12:0 (Figs. 3 and 4). Overexpression of the inactive AtFAAH proteins showed no statistically significant enhancement of growth, while the native AtFAAH overexpressors exhibited ~30 % increase in overall seedling growth when compared to wild-type plants. Moreover, unlike the native AtFAAH overexpressors, none of these site-directed mutant lines showed any significant tolerance to exogenous NAE except that the R307A mutant transformed in wild-type background appeared to grow slightly better than either wild-type or S281/282A mutant in the same background.

*AtFAAH enzyme activity is not required for hypersensitivity to ABA and hypersusceptibility to nonhost pathogens.* We have previously shown that transcript levels of *ABA-insensitive 3* (*ABI3*), a key transcription factor for ABA-responsive genes, are inversely associated with AtFAAH expression levels in Arabidopsis (30). Inconsistent with this observation, overexpression of AtFAAH protein resulted in seedlings that were hypersensitive to ABA despite lower transcript levels of *ABI3* (30). To determine whether NAE hydrolase activity of AtFAAH was required for ABA hypersensitivity observed in AtFAAH overexpressing plants (30), the plants overexpressing the mutant forms of AtFAAH were grown for 10 days in the presence of ABA and their growth phenotypes were determined in detail as described above. Surprisingly, all seedlings expressing S281/282A or R307A mutants, regardless of their backgrounds, still exhibited severe hypersensitivity to ABA to a very similar degree observed for the native AtFAAH overexpressors (Figs. 3 and 4), suggesting that AtFAAH enzyme activity and NAE turnover by the enzyme are not required for the ABA hypersensitivity.

Previous studies showed that the AtFAAH overexpressors had compromised basal resistance and were susceptible to certain nonhost pathogens (31). However, it was not established if the enzyme activity was involved in causing the susceptibility. To check this, plants expressing S281/282A or R307A mutants in both wild-type and *AtFAAH* knockout backgrounds were inoculated with nonhost pathogen as described (31). Development of symptoms on the inoculated leaves was monitored and the bacterial growth was quantified as described in the experimental procedures. Consistent with earlier observations (31), at five days post-inoculation with nonhost pathogen, *P. syringae* pv. *tabaci*, the native AtFAAH overexpressors had chlorotic lesions in most of the infiltrated leaves as compared to Col-0 (Fig. 5A). Interestingly, transgenic plants expressing S281/282A or R307A mutants in both Col-0 and *AtFAAH* knockout backgrounds, showed more chlorotic lesions, similar to those of native *AtFAAH* overexpressors, in most of the infiltrated leaves as compared to Col-0 (Fig. 5A). Consistent with the disease symptoms, there was an increase in bacterial growth at three days post-inoculation in the transgenic plants expressing either native AtFAAH or AtFAAH mutants (S281/282A or R307A) when compared to Col-0 (Fig. 5B).

Collectively, these results indicate that the enhanced growth and the tolerance to exogenous NAE of the native AtFAAH-overexpressing seedlings are attributable to elevated NAE hydrolase activity of AtFAAH protein, whereas the hypersensitivity to ABA and hypersusceptibility to nonhost pathogens of the AtFAAH overexpressors are independent of the catalytic activity of the enzyme but rather

Downloaded from www.jbc.org by guest, on July 11, 2010

dependent on the presence of higher amounts of the protein only.

## DISCUSSION

After "oleamide hydrolase" activity was first affinity-purified from rat liver membranes and the same enzyme was found to display high levels of "anandamide hydrolase" activity (7), FAAH has been intensely investigated in animal systems to uncover its functions in regulating the endocannabinoid signaling system and to develop new therapeutics for the treatment of human disorders (reviewed in (9-10,36)). NAEs in plants are hydrolyzed by a membrane-associated hydrolase functionally analogous to the mammalian FAAH (24-25,27,29), and an Arabidopsis FAAH homologue was identified (24), suggesting that a FAAH-mediated pathway exists in plants as well for the metabolism of endogenous NAEs (reviewed in (37-39)). However, since plant FAAH homologues have been studied only recently, our knowledge on functions of this enzyme in plants is fragmentary and many questions remain to be addressed.

Structure-function relationships for AtFAAH were predicted by homology-based modeling of the plant FAAH AS domain using the rat FAAH three-dimensional structure as a template (25). However no direct experimental evidence other than inhibitor studies has suggested that the plant and animal enzymes operate by a conserved mechanism. And inhibition by serine hydrolase inhibitors cannot distinguish between the Ser-Ser-Lys and the Ser-His-Asp catalytic triads. Here we show that site-directed mutagenesis of five residues conserved in the AS region abolished the amidase activity of AtFAAH, supporting a conserved Ser-Ser-Lys catalytic mechanism. All five residues were predicted to be located in the immediate vicinity of the active site pocket and the putative catalytic residues (K205, S281, and S305) showed nearly direct overlap among all plant and rat FAAH proteins (25).

FAAH has an unusual catalytic feature in that, in addition to amidase activity, it possesses esterase activity at an equivalent rate (32). Among the five catalytically important residues of rat FAAH, R243A mutant was reported to exhibit unaffected esterase activity despite severely compromised amidase activity (19). In contrast to this finding, the corresponding mutant of AtFAAH (R307A) displayed abolished esterase activity in a similar manner to other site-directed mutants tested (Fig. 1E). This noticeable difference between rat and Arabidopsis FAAH indicates that, unlike rat FAAH, the amidase and esterase efficiencies of AtFAAH are functionally and tightly coupled. Another differential catalytic property between animal and plant FAAH enzymes has been previously shown by tolerance of plant FAAH to URB597, a specific inhibitor of animal FAAH (25). Collectively, these findings suggest that although the catalytic mechanism is conserved between the plant and animal enzymes, there are likely subtle differences within the AtFAAH active site that remain to be resolved at the structural level.

In addition to the expected phenotypes of plants overexpressing AtFAAH (e.g., tolerance to exogenous NAEs), these plants exhibited several unexpected phenotypes unable to be explained by NAE hydrolysis, such as hypersensitivity to ABA (30) and enhanced susceptibility to several bacterial pathogens (31). Here we provide experimental evidence that AtFAAH influences Arabidopsis growth and responses to ABA and pathogens through distinctly different molecular mechanisms.

Our previous studies suggested that hydrolysis of endogenous NAEs by the amidase activity of AtFAAH were important for normal Arabidopsis seedling growth (28-29). Here we further support this hypothesis by observing growth phenotype of the plants that overexpress the inactive enzymes. Lack of both enhancement of growth and NAE tolerance by overexpressing inactive AtFAAH proteins reinforces our previous conclusions that FAAH is a modulator of endogenous NAE levels in plants and depletion of NAE by the action of FAAH is one of the key components that participate in the regulation of seedling growth.

Surprisingly, transgenic lines overexpressing S281/282A or R307A mutants of AtFAAH that produced inactive enzyme still exhibited ABA hypersensitivity and hypersusceptibility to nonhost pathogens to a degree similar to the native AtFAAH overexpressors, suggesting that AtFAAH-mediated ABA hypersensitivity and disease susceptibility are independent of catalytic activity of the enzyme toward acylamide or

Downloaded from www.jbc.org by guest, on July 11, 2010

acylester substrates. The disease susceptibility and ABA hypersensitivity of the transgenic plants expressing mutant AtFAAH (S281/282A or R307A) in the *AtFAAH* knockout background is almost similar to overexpressors (Figs. 3 and 5). This can be attributed to the presence of more mutant AtFAAH protein since the expression is constitutively driven by CaMV 35S promoter. Indeed, Western analysis clearly shows more accumulation of mutant proteins in the knockout background (Fig. 2).

We speculate that AtFAAH protein itself might directly interact with other protein(s) involved in ABA and/or defense signaling. We identified two conserved domains near the C-terminus of plant FAAH proteins outside of the catalytic site (25,37) which perhaps could facilitate interactions with target proteins. A recent report indicated that mammalian FAAH can interact with a membrane protein, ERp57, in caveolin-rich membranes (40), but the physiological significance of this interaction remains unclear. Future efforts will be aimed at uncovering the mechanism(s) by which AtFAAH may exert its effects on ABA sensitivity and disease susceptibility by identifying the binding partner molecule(s) of AtFAAH in Arabidopsis cells and identifying domains responsible for interactions.

Alternatively, differential localization of overexpressed FAAH protein (mutant or otherwise) might be responsible for the ABA and pathogen sensitivity phenotypes. However, this explanation is not entirely satisfactory because in previous experiments, when FAAH-GFP was overexpressed in the *faah* knockout background this overexpressed protein complemented the knockout phenotype and conferred tolerance to exogenous NAE in a manner similar to overexpression of FAAH without GFP (31). This suggested that the ER/plasma membrane localization of the FAAH-GFP was at least partially reflective of the normal location of FAAH (to functionally restore the phenotype of knockouts) and that this FAAH-GFP overexpression was a reasonable reporter of overexpressed FAAH location since the NAE-tolerant growth was similar between plants overexpressing either FAAH protein (31). Nonetheless, an effect of FAAH location due to over abundance of active or inactive FAAH transgene product should not be entirely ruled out.

In conclusion, we have shown that the AtFAAH influences plant growth through its hydrolysis of acylethanolamides, but that interactions with ABA and defense signaling are independent of its hydrolytic activity. We proposed previously that NAE metabolism and its influence by FAAH resides at the balance between plant growth and the responses of plants to stress (38). The results presented here are consistent with this concept and offer bifurcating mechanisms that may mediate this physiological control. Although understanding the detailed mechanisms involved in these two processes will require further experimentation beyond the scope of this paper, the novel results presented here provide continued direction to functionally define the group of enzymes that metabolize NAEs in plants. Further, this work suggests the future possibility to uncouple the remarkable increase in overall plant growth seen in AtFAAH overexpressors from the concomitant increased susceptibility to stress which could have important applications in crop biotechnology.

Downloaded from www.jbc.org by guest, on July 11, 2010

## REFERENCES


1. Desarnaud, F., Cadas, H., and Piomelli, D. (1995) *J Biol Chem* **270**, 6030-6035
2. Deutsch, D. G., and Chin, S. A. (1993) *Biochem Pharmacol* **46**, 791-796
3. Schmid, P. C., Zuzarte-Augustin, M. L., and Schmid, H. H. (1985) *J Biol Chem* **260**, 14145-14149
4. Ueda, N., Kurahashi, Y., Yamamoto, S., and Tokunaga, T. (1995) *J Biol Chem* **270**, 23823-23827
5. Cravatt, B. F., Prospero-Garcia, O., Siuzdak, G., Gilula, N. B., Henriksen, S. J., Boger, D. L., and Lerner, R. A. (1995) *Science* **268**, 1506-1509
6. Maurelli, S., Bisogno, T., De Petrocellis, L., Di Luccia, A., Marino, G., and Di Marzo, V. (1995) *FEBS Lett* **377**, 82-86

7. Cravatt, B. F., Giang, D. K., Mayfield, S. P., Boger, D. L., Lerner, R. A., and Gilula, N. B. (1996) *Nature* **384**, 83-87
8. Fowler, C. J. (2006) *Fundam Clin Pharmacol* **20**, 549-562
9. McKinney, M. K., and Cravatt, B. F. (2005) *Annu Rev Biochem* **74**, 411-432
10. Fezza, F., De Simone, C., Amadio, D., and Maccarrone, M. (2008) *Subcell Biochem* **49**, 101-132
11. Chebrou, H., Bigey, F., Arnaud, A., and Galzy, P. (1996) *Biochim Biophys Acta* **1298**, 285-293
12. Patricelli, M. P., Lovato, M. A., and Cravatt, B. F. (1999) *Biochemistry* **38**, 9804-9812
13. Cai, G., Zhu, S., Wang, X., and Jiang, W. (2005) *FEMS Microbiol Lett* **249**, 15-21
14. Gopalakrishna, K. N., Stewart, B. H., Kneen, M. M., Andricopulo, A. D., Kenyon, G. L., and McLeish, M. J. (2004) *Biochemistry* **43**, 7725-7735
15. Labahn, J., Neumann, S., Buldt, G., Kula, M. R., and Granzin, J. (2002) *J Mol Biol* **322**, 1053-1064
16. Neu, D., Lehmann, T., Elleuche, S., and Pollmann, S. (2007) *FEBS J* **274**, 3440-3451
17. Bracey, M. H., Hanson, M. A., Masuda, K. R., Stevens, R. C., and Cravatt, B. F. (2002) *Science* **298**, 1793-1796
18. McKinney, M. K., and Cravatt, B. F. (2003) *J Biol Chem* **278**, 37393-37399
19. Patricelli, M. P., and Cravatt, B. F. (2000) *J Biol Chem* **275**, 19177-19184
20. Cravatt, B. F., Demarest, K., Patricelli, M. P., Bracey, M. H., Giang, D. K., Martin, B. R., and Lichtman, A. H. (2001) *Proc Natl Acad Sci U S A* **98**, 9371-9376
21. Clement, A. B., Hawkins, E. G., Lichtman, A. H., and Cravatt, B. F. (2003) *J Neurosci* **23**, 3916-3923
22. Cravatt, B. F., Saghatelian, A., Hawkins, E. G., Clement, A. B., Bracey, M. H., and Lichtman, A. H. (2004) *Proc Natl Acad Sci U S A* **101**, 10821-10826
23. Lichtman, A. H., Shelton, C. C., Advani, T., and Cravatt, B. F. (2004) *Pain* **109**, 319-327
24. Shrestha, R., Dixon, R. A., and Chapman, K. D. (2003) *J Biol Chem* **278**, 34990-34997
25. Shrestha, R., Kim, S. C., Dyer, J. M., Dixon, R. A., and Chapman, K. D. (2006) *Biochim Biophys Acta* **1761**, 324-334
26. Chapman, K. D., Tripathy, S., Venables, B., and Desouza, A. D. (1998) *Plant Physiol* **116**, 1163-1168
27. Shrestha, R., Noordermeer, M. A., van der Stelt, M., Veldink, G. A., and Chapman, K. D. (2002) *Plant Physiol* **130**, 391-401
28. Blancaflor, E. B., Hou, G., and Chapman, K. D. (2003) *Planta (Berlin)* **217**, 206-217
29. Wang, Y. S., Shrestha, R., Kilaru, A., Wiant, W., Venables, B. J., Chapman, K. D., and Blancaflor, E. B. (2006) *Proc Natl Acad Sci U S A* **103**, 12197-12202
30. Teaster, N. D., Motes, C. M., Tang, Y., Wiant, W. C., Cotter, M. Q., Wang, Y. S., Kilaru, A., Venables, B. J., Hasenstein, K. H., Gonzalez, G., Blancaflor, E. B., and Chapman, K. D. (2007) *Plant Cell* **19**, 2454-2469
31. Kang, L., Wang, Y. S., Uppalapati, S. R., Wang, K., Tang, Y., Vadapalli, V., Venables, B. J., Chapman, K. D., Blancaflor, E. B., and Mysore, K. S. (2008) *Plant J* **56**, 336-349
32. Patricelli, M. P., and Cravatt, B. F. (1999) *Biochemistry* **38**, 14125-14130
33. Ghafouri, N., Tiger, G., Razdan, R. K., Mahadevan, A., Pertwee, R. G., Martin, B. R., and Fowler, C. J. (2004) *Br J Pharmacol* **143**, 774-784
34. Fowler, C. J., Jonsson, K. O., and Tiger, G. (2001) *Biochem Pharmacol* **62**, 517-526
35. Clough, S. J., and Bent, A. F. (1998) *Plant J* **16**, 735-743
36. Labar, G., and Michaux, C. (2007) *Chem Biodivers* **4**, 1882-1902
37. Chapman, K. D. (2004) *Prog Lipid Res* **43**, 302-327
38. Kilaru, A., Blancaflor, E. B., Venables, B. J., Tripathy, S., Mysore, K. S., and Chapman, K. D. (2007) *Chem Biodivers* **4**, 1933-1955
39. Gertsch, J. (2008) *Planta Med* **74**, 638-650
40. Yates, M. L., and Barker, E. L. (2007) *FASEB J* **21**, 885.1

Downloaded from www.jbc.org by guest, on July 11, 2010

## FOOTNOTES

*This work was supported by the Samuel Roberts Noble Foundation and a grant from the Office of Science (BES, agreement no. DE-FG02-05ER15647), U.S. Department of Energy to EBB and KDC.

The abbreviations used are: FAAH, fatty acid amide hydrolase; NAE, *N*-acylethanolamine; ABA, abscisic acid; AtFAAH, *Arabidopsis thaliana* FAAH; AS, amidase signature; ABI, ABA-insensitive; 2-AG, *sn*-2-arachidonyl glycerol; CaMV, cauliflower mosaic virus; DMSO, dimethylsulfoxide; KO, knockout; OE, overexpressor; SW, S281/282A mutant expressed in wild-type background; RW, R307A mutant expressed in wild-type background; SK, S281/282A mutant expressed in *AtFAAH* knockout background; RK, R307A mutant expressed in *AtFAAH* knockout background; Ni-NTA, nickel-nitrilotriacetic acid; DDM, *n*-dodecyl β-D-maltoside; PVDF, polyvinylidene fluoride; FFA, free fatty acid; URB597, 3'-carbamoyl-biphenyl-3-yl-cyclohexylcarbamate.

## FIGURE LEGENDS

**Figure 1. Expression of site-directed AtFAAH mutants in *E. coli* and evaluation of their enzyme activities.** (A) Conserved catalytic residues in the amidase signature (AS) sequence between rat and Arabidopsis FAAH proteins. Full sequences of rat and Arabidopsis FAAH (Ara) were aligned using T-coffee software (Swiss Institute of Bioinformatics). AS regions that consist of 125 amino acids are shown here. Five residues (K142, S217, S218, S241, and R243) known to be critical for rat FAAH activity are highlighted in black boxes. These residues are also conserved in Arabidopsis sequence as shown (K205, S281, S282, S305, and R307). (B) Western blot analysis. Wild-type AtFAAH protein without mutation (WT) and the proteins with site-directed mutation (indicated by their corresponding residues) were expressed in *E. coli*, and affinity-purified proteins (1 μg) were analyzed by Western blot. All mutated AtFAAH proteins were immunolocalized at the position expected (~69.4 kDa including epitope tags). (C) Representative radiochromatograms for NAE hydrolase assay. Equal amounts of affinity-purified proteins were reacted with [1-$^{14}$C]NAE16:0. Total lipids extracted from reaction mixtures were separated by thin layer chromatography (TLC) and analyzed by radiometric scanning. Each radiochromatogram shows the distance (mm) on x-axis that lipids migrated on the TLC plate and their radioactivity (cpm) on y-axis. Picks that represent NAE and FFA (free fatty acid) are indicated. Wild-type (WT) and S360A mutant show a significant production of FFA (peak at ~97 mm), whereas all mutants did not produce any detectable products. Enzyme activities for mutants compared to wild-type are summarized in Table 1. (D) Kinetic comparison of wild-type and S360A mutant. Initial velocities (for 10 min) were measured at increasing concentrations of [1-$^{14}$C]NAE16:0. Michaelis-Menten plot and Lineweaver-Burk plot are shown here for comparison. Plots were generated with Prism software v3.0 (GraphPad Software, San Diego, CA). Data points represent means ± S.D. of triplicate assays. Kinetic parameters for wild-type and S360A mutant are summarized in Table 2. (E) Lack of enzyme activity of the mutants toward monoacylester and primary amide substrates. 1 μg of purified wild-type and S360A proteins and 10 μg of all other mutant proteins were reacted with 2-arachidonoyl glycerol (2-AG; left plate) and 9-octadecenamide (oleamide; right plate). Total lipids from the reactions were separated by TLC, and visualized by iodine vapors. Positions for substrates (2-AG and oleamide) and products (arachidonic acid and oleic acid) are indicated on left. Wild-type (WT) and S360A mutant show a significant formation of FFA products, whereas all mutants display essentially no product formation. Arachidonic acid and oleic acid standards (Std.) are also included for position comparison.

**Figure 2. Expression of site-directed AtFAAH mutants in Arabidopsis and evaluation of their enzyme activities.** (A) Western blot analysis. Arabidopsis wild-type (WT) and transgenic lines (SW, RW, OE, KO, SK, and RK) were grown for 10 days as described in the experimental procedures. Total proteins (200 μg) from each of seedling homogenates were analyzed by Western blot. All AtFAAH

Downloaded from www.jbc.org by guest, on July 11, 2010

proteins of overexpressors (SW, RW, OE, SK, and RK) were immunolocalized at the position expected (~66.1 kDa). SW, S281/282A mutant expressed in wild-type background. RW, R307A mutant expressed in wild-type. OE, native AtFAAH overexpressor. KO, *AtFAAH* T-DNA insertion knockout. SK, S281/282 mutant expressed in *AtFAAH* knockout background. RK, R307A mutant expressed in *AtFAAH* knockout. (B) NAE hydrolysis activities. Total proteins (50 μg) from each of 10-day old seedling homogenates were reacted with [1-$^{14}$C]NAE16:0. Total activities (μmol/h) were measured based on radioactivity of the product formed. All AtFAAH overexpressors with site-directed mutation (SW, RW, SK, and RK) exhibited significantly lower NAE hydrolase activity than the native AtFAAH overexpressor (OE). The error bars represent S.D. from triplicate measurements. Asterisks indicate a significant difference ($p < 0.0001$) compared with OE, which was determined by Student's *t*-test.

**Figure 3. Overall apparent growth phenotype of Arabidopsis seedlings expressing AtFAAH mutants in response to NAE and ABA.** Seedlings were grown for 10 days in the presence of DMSO only, 30 μM NAE12:0, or 0.25 μM ABA (A) Growth phenotype in liquid media. Seedlings were grown in flasks, and then transferred onto petri dishes to photograph. Representative images of triplicate experiments are shown here. All site-directed mutant lines (SW, RW, SK, and RK) display no growth enhancement and no NAE tolerance compared to native AtFAAH overexpressor (OE), whereas they all show ABA hypersensitivity compared to their background lines (WT and KO). (B) Growth phenotype in solid media. Representative images of 24 individual seedlings for each line are shown here. Note that relative growths of the different lines are highly analogous to those in liquid media (A).

**Figure 4. Quantitative growth measurements of Arabidopsis seedlings expressing AtFAAH mutants in response to NAE and ABA.** 10-day old seedlings were quantified in terms of seedling fresh weight (mg seedling tissue per mg seed sown), primary root length (cm), and cotyledon area ($mm^2$). Values for fresh weight represent means ± S.D. of triplicate measurements. Values for primary root length and cotyledon area represent means ± S.D. of 10 individual seedlings. Single and double asterisks indicate a significant difference ($p < 0.0001$) compared with wild-type (WT) and *AtFAAH* knockout (KO), respectively, which was determined by Student's *t*-test.

**Figure 5. Enhanced growth of nonhost pathogen *P. syringae* pv. *tabaci* in Arabidopsis expressing AtFAAH mutants.** (A) Leaves were syringe-infiltrated with bacteria of a concentration of $5 \times 10^7$ cfu/mL for symptom development. The disease symptoms were photographed at 5 days post-inoculation (DPI). Inoculated leaves are indicated by arrows. (B) Plants were vacuum-infiltrated with bacteria of a concentration of $10^7$ cfu/mL for growth assays. Bacterial growth was quantified at 3 DPI (white bars), and at 0 DPI (black bars) for comparison. The error bars represent S.D. from triplicate measurements. Asterisks indicate a significant difference ($p < 0.0001$) compared with wild-type (WT; 3 DPI), which was determined by Student's *t*-test.

Downloaded from www.jbc.org by guest, on July 11, 2010

**Table 1. NAE hydrolysis activity of mutant proteins expressed in *E. coli*.** Proteins affinity-purified from *E. coli* were reacted with $^{14}$C-radiolabeled NAE12:0, NAE16:0, or NAE18:0. Specific activities were calculated based on radioactivity of the products formed. Values are shown as means ± S.D. of triplicate measurements. For each NAE substrate, enzyme activities relative to wild-type AtFAAH without mutation (100 %; WT) are indicated under "relative activity".

| Enzymes | Specific activity | | | Relative activity | | |
|---|---|---|---|---|---|---|
| | NAE12:0 | NAE16:0 | NAE18:2 | NAE12:0 | NAE16:0 | NAE18:2 |
| | μmol $h^{-1}mg^{-1}$ | | | % | | |
| WT | 117±8 | 134±10 | 139±8 | 100 | 100 | 100 |
| K205A | 0.06±0.01 | 0.07±0.02 | 0.10±0.02 | 0.05 | 0.05 | 0.07 |
| S281/282A | 0.08±0.01 | 0.08±0.01 | 0.09±0.01 | 0.07 | 0.06 | 0.06 |
| S305A | 0.09±0.02 | 0.11±0.02 | 0.15±0.01 | 0.08 | 0.08 | 0.11 |
| R307A | 0.16±0.03 | 0.21±0.03 | 0.34±0.05 | 0.14 | 0.16 | 0.24 |
| S360A | 119±7 | 145±12 | 152±11 | 102 | 108 | 109 |

**Table 2. Apparent kinetic parameters of wild-type AtFAAH and S360A mutant.** Initial velocities (for 10 min) of affinity-purified wild-type (WT) and S360A proteins were measured at increasing concentrations of [1-$^{14}$C]NAE16:0. Values were estimated with Prism software v3.0 (GraphPad Software, San Diego, CA) from triplicate measurements.

| Enzymes | $V_{max}$ | $K_m$ | $K_{cat}$ | $K_{cat}/K_m$ |
|---|---|---|---|---|
| | $\mu mol\ h^{-1}mg^{-1}$ | $\mu M$ | $s^{-1}$ | $\mu M^{-1}s^{-1}$ |
| WT | 181.7 | 23.0 | 3.33 | 0.145 |
| S360A | 205.4 | 33.1 | 3.77 | 0.114 |

Figure 1.

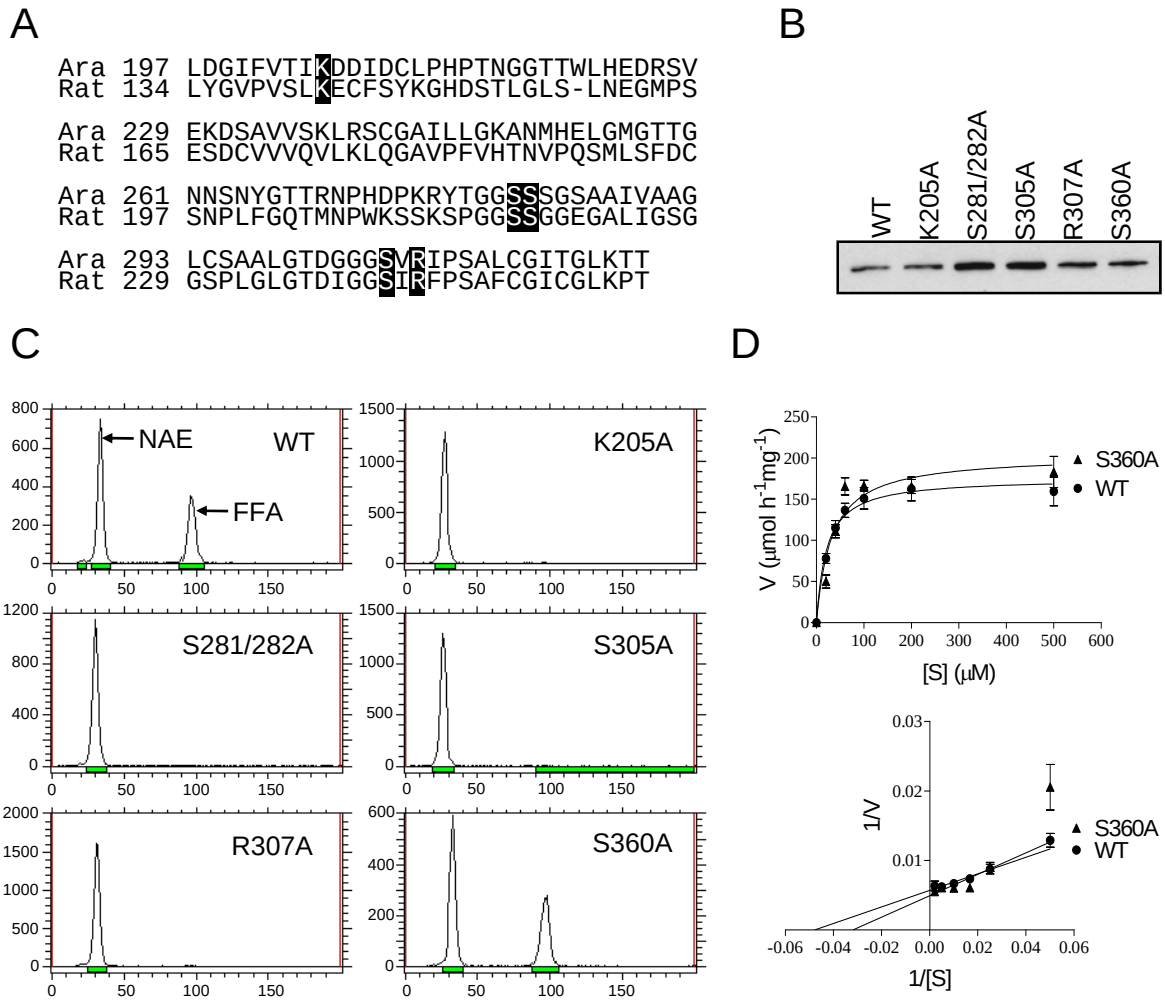
A
Ara 197 LDGIFVTIKDDIDCLPHPTNGGTTWLHEDRSV
Rat 134 LYGVPVSLKECFSYKGHDSTLGLS-LNEGMPS
Ara 229 EKDSAVVSKLRSCGAILLGKANMHELGMGTTG
Rat 165 ESDCVVVQVLKLQGAVPFVHTNVPQSMLSFDC
Ara 261 NNSNYGTTRNPHDPKRYTGGSSSGSAAIVAAG
Rat 197 SNPLFGQTMNPWKSSKSPGGSSGGEGALIGSG
Ara 293 LCSAALGTDGGGSVRIPSALCGITGLKTT
Rat 229 GSPLGLGTDIGGSIRFPSAFCGICGLKPT
B
WT
K205A
S281/282A
S305A
R307A
S360A
C
NAE
FFA
WT
K205A
S281/282A
S305A
R307A
S360A
D
V (µmol h-1mg-1)
[S] (µM)
S360A
WT
1/V
1/[S]
S360A
WT
E
Std.
WT
K205A
S281/282A
S305A
R307A
S360A
Arachidonic acid
2-AG
Std.
WT
K205A
S281/282A
S305A
R307A
S360A
Oleic acid
Oleamide

Figure 2.

A

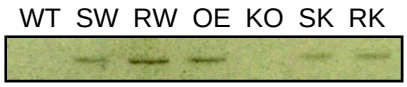
WT SW RW OE KO SK RK

B

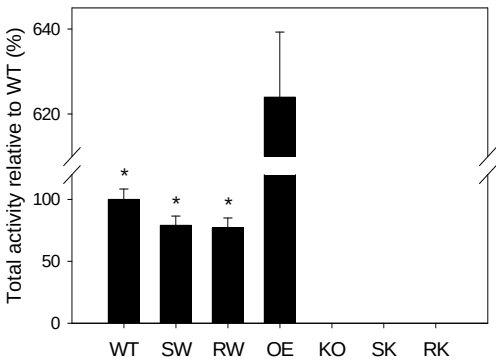
Total activity relative to WT (%)
640
620
100
50
0
*
*
*
WT SW RW OE KO SK RK

Figure 3.

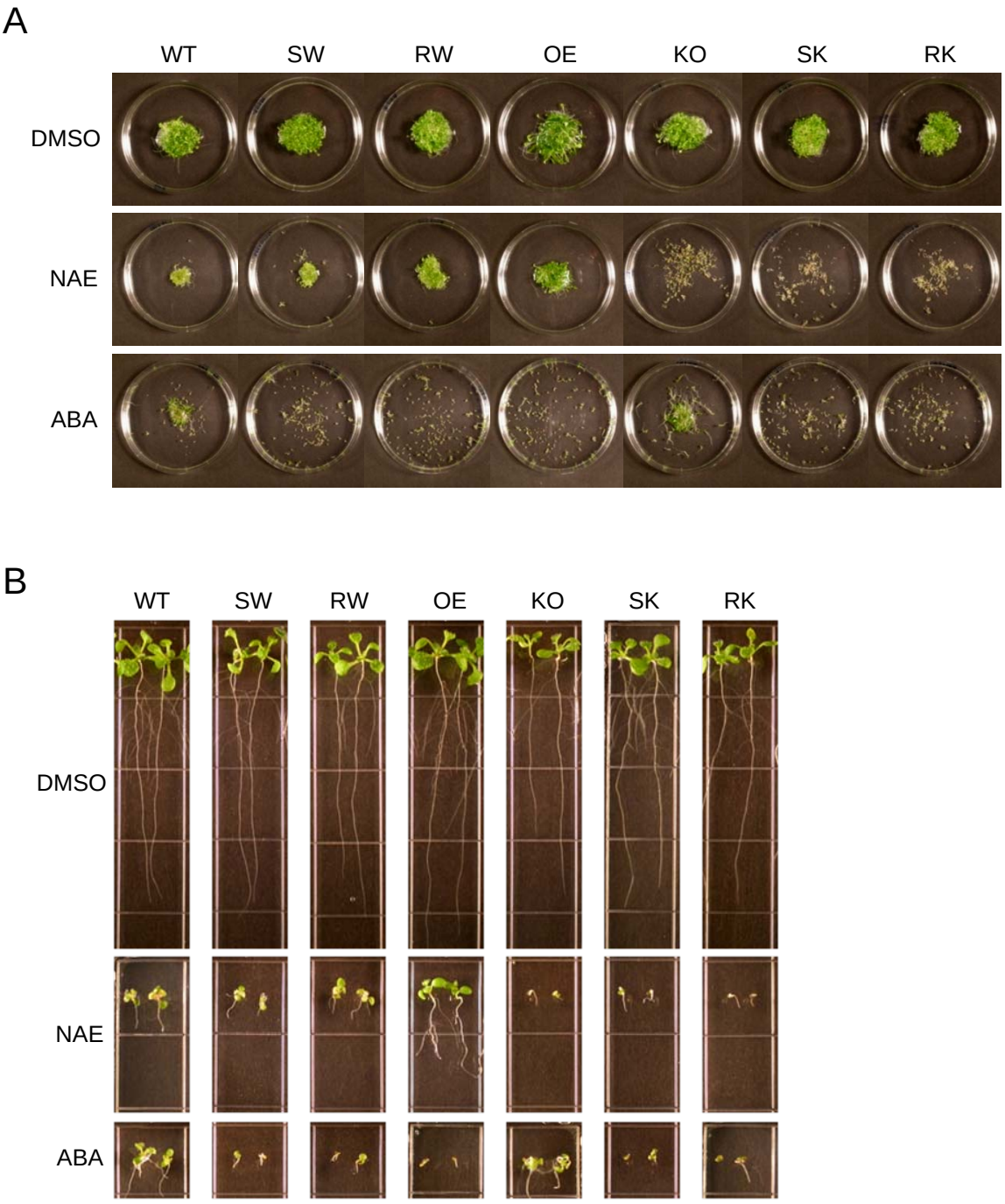
A
WT
SW
RW
OE
KO
SK
RK
DMSO
NAE
ABA
B
WT
SW
RW
OE
KO
SK
RK
DMSO
NAE
ABA

Figure 4.

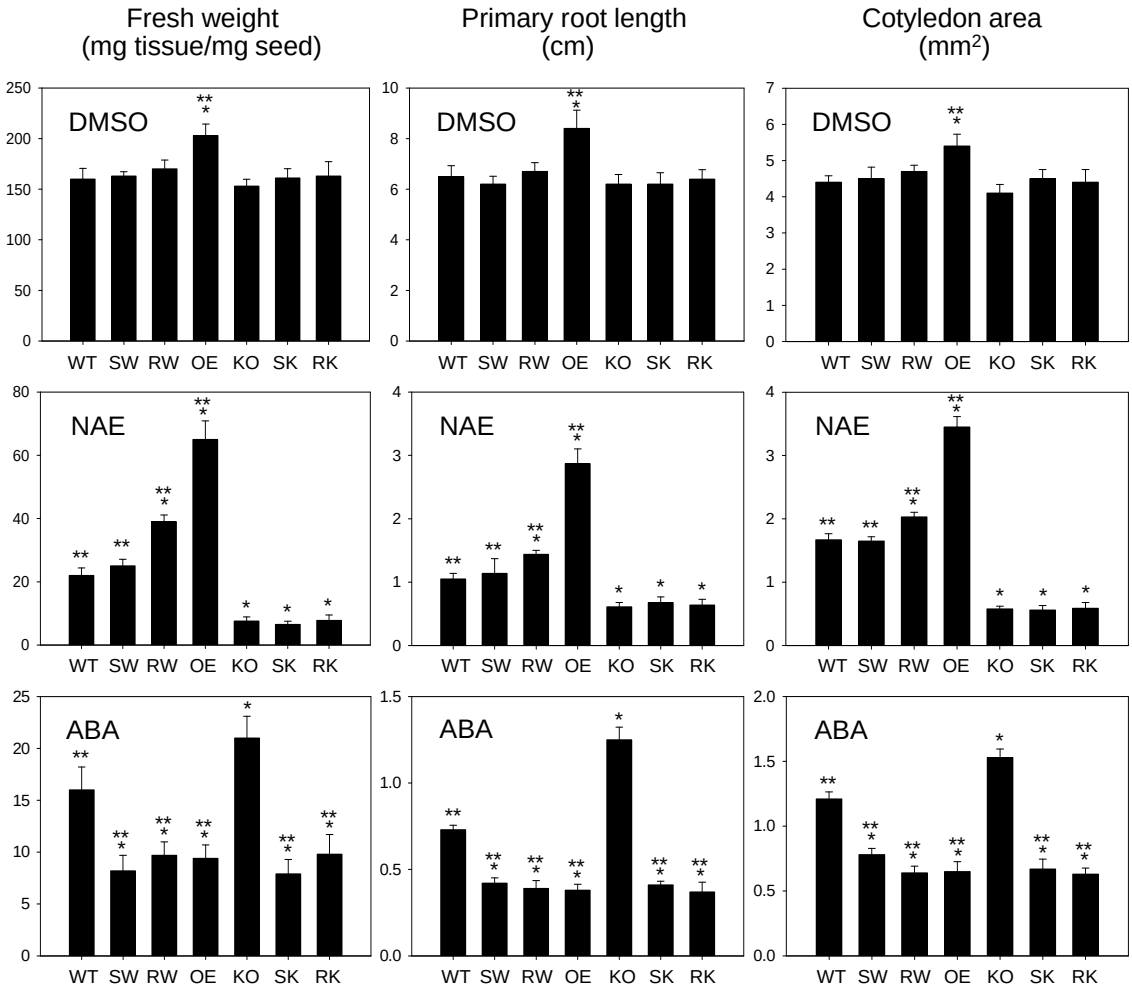
Fresh weight
(mg tissue/mg seed)
Primary root length
(cm)
Cotyledon area
(mm2)
DMSO
NAE
ABA
WT SW RW OE KO SK RK

Figure 5.

A

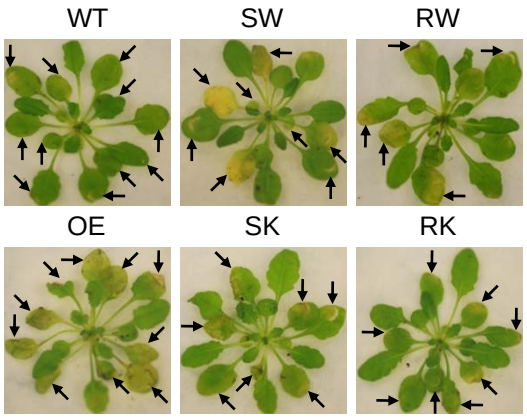
WT
SW
RW
OE
SK
RK

B

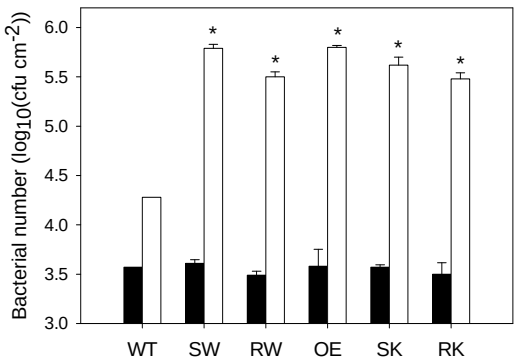
Bacterial number (log10(cfu cm-2))
6.0
5.5
5.0
4.5
4.0
3.5
3.0
*
WT
SW
RW
OE
SK
RK